RSC Advances

PAPER

View Article Online
View Journal | View Issue

Check for updates

Cite this: *RSC Adv.*, 2024, **14**, 17547

Comprehensive assessment of enhancing dewaterability of dredged sediments by starch-based flocculant

Shilei Tang, Shaobin Huang, * Pengfei Chen, Zhipeng Wu and Tianyu Zhao

Received 22nd March 2024
Accepted 25th May 2024

DOI: 10.1039/d4ra02189d

rsc.li/rsc-advances

Dredged sediment poses significant challenges for transportation and subsequent treatment due to its high water content and large volume. Coagulation, a common method of dewatering, can significantly enhance the dewatering performance of dredged sediment. This study synthesized a cationic starch-based flocculant [starch-3-chloro-2-hydroxypropyl trimethylammonium chloride (St-CTA)] through etherification for the flocculation dewatering of dredged sediment. The effectiveness and mechanism of St-CTA as a dewatering flocculant for dredged sediment were investigated. The results demonstrated that when the dosage of St-CTA was 12 mg g^{-1} TSS (total suspended solids), the dehydration property of dredged sediment substantially improved, with the specific resistance to filtration (SRF) decreasing by 93.3%, the capillary suction time (CST) by 93.5%, and the water content of the filter cake (WC) by 9.7%. The removal rate of turbidity of the supernatant from the conditioned dredged sediment reached 99.6%, accelerating the settling speed and effectively capturing and separating fine particles from the sediment. St-CTA significantly increased the median particle size (D50), altered the microstructure and extracellular polymeric substances (EPS) of the flocs, and increased the fractal dimension of the flocs, making them more compact and conducive to the formation of drainage channels. These findings confirm the feasibility of using potentially environmentally friendly St-CTA as a rapid dewatering conditioning agent for sediment.

Open Access Article. Published on 31 May 2024. Downloaded on 1/31/2026 4:51:15 PM.
This article is licensed under a Creative Commons Attribution-NonCommercial 3.0 Unported Licence.

1 Introduction

Sediment is an integral part of aquatic systems, but with the advancement of industrialization, it has become increasingly contaminated.[1] As a result of microbial activity, organic matter in sediments is decomposed, which reduces the dissolved oxygen content in the water and generates gaseous pollutants such as ammonia and hydrogen sulfide.[2] Environmental dredging has emerged as an effective method to mitigate sediment accumulation.[3] However, in recent years, environmental dredging operations have generated a large amount of dredged sediment containing water and mud blocks, which will cause secondary pollution if not effectively treated.[4,5] Characterized by high water content and large volume, dredged sediment presents challenges for traditional dredging sites, including extensive area requirements and prolonged processing times.[6] Therefore, the subsequent disposal of dredged sediment has become a hot issue in environmental protection. Dredged sediment holds potential application value, with subsequent management options including land use, composting, and the production of construction materials.[7] However, the high water content of dredged sediment makes the secondary utilization of sediment face severe challenges.[8] Therefore, dehydration is essential in minimizing the volume of dredged sediment and facilitating storage and transportation.[9]

The main pretreatment methods for dredging sediment dehydration include physical and chemical methods. Among them, the physical methods include plate-frame pressure filtration, centrifugation, geotextile bag dehydration, *etc.*, and the chemical methods include coagulation, electrochemistry, surfactants, acid-base dehydration.[10–13] The water in dredged sediment consists of free water and bound water.[14] Given the complex composition of sediment and its difficulty in dewatering, the physical methods often only remove a portion of the free water in the sediment. Chemical processes can promote the conversion of bound water to free water, thereby removing some of the bound water.[10] In general, a combination of physical and chemical methods yields higher dewatering efficiency. Coagulation is one of the most mature chemical dehydration methods. Coagulants include inorganic, organic, and biological coagulants.[15] Commonly used inorganic coagulants include aluminum salts and iron salts, while organic coagulants include polypropylene and polyethylene substances. The mechanism of their flocculation is double layer compression, adsorption and charge neutralization, and adsorption bridging.[16] However, conventional coagulants can produce additional pollution. For

School of Environment and Energy, South China University of Technology, Higher Education Mega Center, Guangzhou 510006, P. R. China. E-mail: chshuang@scut.edu.cn

© 2024 The Author(s). Published by the Royal Society of Chemistry

Open Access Article. Published on 31 May 2024. Downloaded on 1/31/2026 4:51:15 PM. This article is licensed under a Creative Commons Attribution-NonCommercial 3.0 Unported Licence.

example, aluminum and ferric salt coagulants can alter the pH of the system, and residual metal ions can corrode sediment treatment equipment. Polyacrylamide coagulants can degrade into acrylamide, which is a potential carcinogen.[17,18] Consequently, natural polymeric organic coagulants with more environmentally friendly and biodegradable properties have become an ideal alternative to traditional coagulants.[19,20] However, natural materials often have disadvantages, such as poor water solubility and low charge density. Further chemical modification of natural polymer material is needed to improve its coagulation effect.[21] Common chemical modification methods include etherification, graft copolymerization, and esterification. Starch, a common natural polymer compound, is widely sourced and cost-effective, making it applicable in many industrial productions.[22] Starch itself cannot be directly used as a flocculant, but its anhydrous glucose units are easy to modify, and the stability of modified starch is excellent,[23] which makes it often used as starch-based flocculants applied in wastewater treatment. However, research on starch-based flocculants is more focused on the application of graft-type or inorganic–organic composite conditioners, and etherified starch flocculants are relatively less studied.[24–28] It should not be ignored that grafting copolymerized starch has higher costs, greater preparation difficulty, and poorer water solubility, while etherized starch has a rigid linear structure and smaller steric hindrances. This means that etherized starch is more conducive to promoting the formation of tiny particles into dense flocs.[25] Etherified starch can also serve as an excellent flocculant. Considering the dredged sediment particles are negatively charged, it is necessary to modify the starch by cationization. Common cationic groups include amino, phosphorus, ammonium, and sulfanilamide. According to relevant reports, with the increase of cationic starch substitution degree, the flocculation effect is further improved due to the enhancement of electrical neutralization.[29] In addition, cationic starch has an excellent bactericidal effect.[30] Compared to traditional inorganic flocculants such as alum and ferric salts, and other synthetic polymeric flocculants, cationic starch, a modified natural starch-based product, reduces reliance on harmful chemicals. It inherently possesses lower toxicity and is closer to its natural state, making it more readily biodegradable by environmental microorganisms. This enhances its biocompatibility, presenting a potentially environmentally friendly alternative in flocculation processes. However, only a few studies on etherified starch in the dewatering of dredged sediment have been reported.

This paper focuses on exploring the feasibility of the application of etherified starch-based flocculants to improve the dehydration property of dredged sediment. A cationic starch with a high substitution degree [starch-3-chloro-2-hydroxypropyl trimethylammonium chloride (St-CTA)] was synthesized as a flocculant for conditioning dredged sediment. The study examined the impact of different dosages of cationic starch on the sediment's dewatering performance by observing changes in CST, SRF, and WC. In addition, according to determining the variety of pH, particle size, rheology, sedimentation rate, turbidity of supernatant, zeta potential, EPS, fractal dimension, and microscopic morphology of dredged sediment, the mechanism of cationic starch affecting the dewatering performance of dredged sediment was discussed.

2 Experimental

2.1 Materials

The dredged sediment samples utilized in this study were collected from the bottom of a river named "Ershayong," which flows through the vicinity of South China University of Technology. The sediment samples were stored in a refrigerator at 4 degrees Celsius and analyzed within three days. Characteristics of the sediment samples can be found in Table 1. Potato starch was purchased from Hualu Food Co., Ltd (Suzhou, China). 3-Chloro-2-hydroxypropyl trimethylammonium chloride (CTA, 65 wt% in water) was provided by Macklin Co., Ltd (Shanghai, China). Sodium hydroxide (NaOH), acetic acid ($C_2H_4O_2$), isopropyl alcohol (C_3H_8O), and other analytical pure chemicals and reagents were purchased from Aladdin Co., Ltd (Shanghai, China).

2.2 Synthesis and characterization of St-CTA

The synthesis of St-CTA was based on methods described in previous literature.[30] Fig. 1 depicts the synthetic route of St-CTA. To synthesize St-CTA, 73 g of potato starch, 180 ml of anhydrous isopropanol, and 38 g of sodium hydroxide solution (40 wt% in water) were placed in a three-neck flask. The temperature of the mixture was raised to 50 °C while stirring continuously. After alkalinizing for one hour, an additional 100 ml of anhydrous isopropanol and 38 g of sodium hydroxide solution were added, along with 130 g of 3-chloro-2-hydroxypropyl trimethylammonium chloride solution (65 wt% in water). The temperature was increased to 70 °C and stirring was maintained for another two hours until the reaction concluded. The reaction mixture was then transferred to a clean large beaker, neutralized with hydrochloric acid *via* titration, and washed several times with anhydrous isopropanol. The system was vacuum filtered and the residue was dried in a freeze vacuum dryer for 48 hours. The dried sample was then ground to obtain the final product, St-CTA. The product was characterized using a Fourier infrared spectroscopy (FTIR, iS50, USA), an elemental analyser (UNICUBE, GER) and ^{1}H nuclear magnetic resonance (^{1}H NMR, Bruker Ascend 600, GER) spectroscopy. D_2O was used as the solvent in NMR experiment. The flocculation experiments were

Table 1 Characteristics of the raw dredged sediment samples[a]

Parameter	Value
SRF (m kg^{-1})	4.21×10^{12}
CST (S)	92.4
Water content (%)	92.1
Zeta potential (mV)	−13.6
pH	7.6
VSS/TSS (%)	14.8

[a] VSS: volatile suspended solids, TSS: total suspended solids.

© 2024 The Author(s). Published by the Royal Society of Chemistry

Open Access Article. Published on 31 May 2024. Downloaded on 1/31/2026 4:51:15 PM.
This article is licensed under a Creative Commons Attribution-NonCommercial 3.0 Unported Licence.

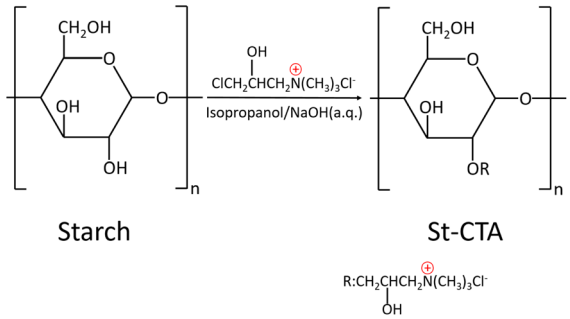

Fig. 1 Synthesis of St-CTA.

conducted to compare the capabilities of starch and St-CTA in enhancing the filterability of sediment. Details of the flocculation process are described in Section 2.3.

2.3 Sediment conditioning procedures

A thoroughly mixed 100 ml sample of dredged sediment was transferred to a 250 ml beaker and stirred using a mechanical stirrer. The mixture was then treated with varying amounts of St-CTA. The stirring protocol was as follows: the sample was stirred at 200 rpm for 2 minutes, followed by stirring at 50 rpm for 5 minutes. After stirring, the sample was tested after 30 minutes of reaction. Each dewatering experiment was repeated thrice.

2.4 Determination of dredged sediment dewatering performance

The dewatering performance of sediment can be measured by specific resistance of filtration (SRF), capillary water absorption time (CST), and filter cake water content (WC).[31,32] The CST of sediment was measured by a capillary water absorption meter (HDFC-10A, CN), and 5 ml of conditioned sediment was sampled for each measurement. The value of SRF can be obtained by eqn (1)

$$\mathrm{SRF} = \frac{2PA^2b}{\mu\omega} \quad (1)$$

where SRF (m kg^{-1}) denotes the specific resistance to the filtration of dredge sediment, P (N m^{-2}) denotes the applied pressure, A (m^2) denotes the area of filter cake, μ (N s m^{-2}) denotes the viscosity of filtrate, ω (kg m^{-3}) denotes the mass of dry solids per volume of dredged sediment on the filtrate medium, which is regarded as a constant, b (s m^{-6}) is calculated by the slope of volume and time of filtrate discharge. One hundred milliliters of the conditioned dredged sediment suspension was filtered with a 0.45 μm filter membrane in a Buchner funnel at a constant pressure of 0.08 MPa until the vacuum was broken. If the vacuum remained undisturbed for 20 minutes, the filtration process would cease, and the final volume of the filtrate would be recorded. The filtrate volume was recorded every 15 seconds. Calculated the water content (WC) of the filter cake after drying the filtered sediment at 105 °C for 24 hours.[33]

2.5 Determination of EPS, particle sizes and microstructure

Initially, thirty milliliters of sediment was centrifuged in a 50 ml tube at 4000 g for 10 minutes, with the resultant supernatant considered as soluble extracellular polymeric substances (S-EPS). The loosely bound EPS (LB-EPS) and tightly bound EPS (TB-EPS) were extracted using an improved hot-extraction method.[34] The organic content in each EPS fraction was analyzed using a fluorescence spectrophotometer (F-7000, Hitachi, Japan). The scanning speed was set at 12 000 nm min^{-1}. Excitation wavelengths ranged from 200 to 400 nm, with an increment of 5 nm, while emission wavelengths ranged from 250 to 550 nm, also with an increment of 5 nm. The photomultiplier tube voltage was maintained at 400 V. The particle size distribution of the conditioned sediment was measured using a laser particle size analyzer (Malvern Mastersizer 3000, UK). After drying the conditioned sediment in a freeze vacuum dryer at −60 °C for 72 hours, its microstructure was examined using a scanning electron microscope (JSM-7600F, Japan).

2.6 Calculation of fractal dimension of floc

The fractal dimension (D_f) of the sediment flocs was calculated using a combination of fractal theory and image analysis.[35] Carefully extracted conditioned sediment was placed in a Petri dish and photographed using a microscope camera (MD30, CN). The obtained images were processed with Image-Pro Plus 6.0 software to identify the projected area (A) and perimeter (P) of the flocs. These parameters were used to calculate the fractal dimension of the flocs, satisfying eqn (2) and (3)

$$A = \alpha P^{D_f} \quad (2)$$

$$\mathrm{Log\ A} = D_f \log P + \log \alpha \quad (3)$$

where α is a dimensionless proportionality constant.

2.7 Other indicators

After the conditioned sediment had settled for 30 minutes, the supernatant was carefully collected using a pipette and its turbidity was measured using a turbidimeter (WZB-175, CN). A 100 ml sample of the mixed conditioned sediment was then placed in a 100 ml graduated cylinder for a sedimentation experiment. The mud–water interface was recorded every 30 seconds for 15 minutes to construct the sedimentation curve of the dredged sediment. The pH of the conditioned sediment was measured using a pH meter (PHS-3E, CN).

3 Results and discussion

3.1 Characterization of St-CTA

Compared with the FTIR spectrum of starch, as shown in Fig. 2a, the spectrum of St-CTA displayed a new peak at 1481 cm^{-1}, which was attributed to the vibrational absorption of the C–H bonds in the quaternary ammonium groups of CTA.[36] Furthermore, the peak near 1010 cm^{-1} in the native starch, attributed to the characteristic C–O–C stretching, shifted

Open Access Article. Published on 31 May 2024. Downloaded on 1/31/2026 4:51:15 PM.
This article is licensed under a Creative Commons Attribution-NonCommercial 3.0 Unported Licence.

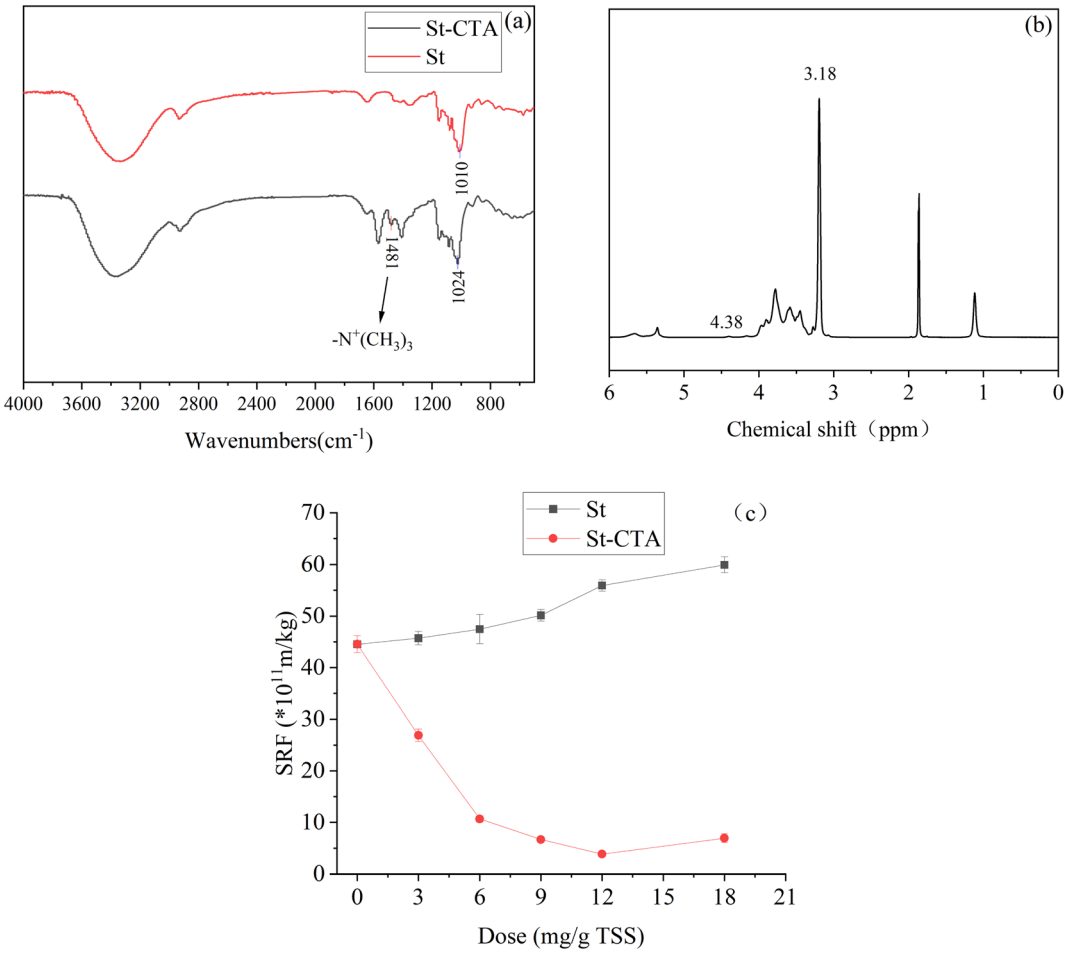

Fig. 2 (a) FTIR spectra of starch (St) and St-CTA; (b) ^{1}H NMR spectrum of St-CTA; (c) variation in specific resistance of sediment conditioned with starch (St) and St-CTA.

to 1024 cm^{-1} in St-CTA. This shift was likely due to the formation of new C–O–C bonds, specifically hydroxypropyl ether bonds, in the modified starch. In the ^{1}H NMR spectra (Fig. 2b), St-CTA showed characteristic peaks at chemical shifts of 3.18 and 4.38 ppm. These were attributed to the methyl protons on the quaternary ammonium groups and the –CH– protons in the hydroxypropyl ether bonds, respectively.[30] These results indicated the successful introduction of quaternary ammonium groups onto the starch molecule. Elemental analysis determined an increase in nitrogen (N) content by 2.03% in St-CTA compared to the native starch. The degree of substitution (DS) of St-CTA was calculated as 30.2%.

Further experiments compared the conditioning effects of starch and modified starch (St-CTA) on enhancing the filtration performance of sediment. As shown in Fig. 2c, the addition of native starch consistently deteriorated the filtration performance of the sediment. In contrast, St-CTA significantly improved the filtration characteristics. The high viscosity of starch, particularly at higher concentrations, likely contributed to an increase in overall sediment viscosity. Moreover, the addition of starch molecules increased the specific resistance of the sediment. This increase is attributed to the poor solubility of native starch in cold water, which may prevent starch particles from fully dissolving, leading to the formation of microparticles that could clog the pores of the filter cloth, further worsening the filtration performance. After modification into St-CTA, the water solubility of the starch improved, allowing its molecular chains to effectively unfold in solution. The quaternary ammonium groups in the St-CTA chains could effectively neutralize the negative charges in the sediment, aiding in bridging and flocculating the sediment particles. These results indicated that etherification modification of potato starch could enhance its flocculating ability and stability. The following sections will delve deeper into the impact of St-CTA on sediment dewatering performance and its associated properties.

3.2 Dose effects of St-CTA on the dewatering performance of dredged sediment

Fig. 3 shows the SRF, CST, and WC of dredged sediment at different St-CTA additions. With the increase of St-CTA dosage from 0 to 12 mg g^{-1} TSS and then to 18 mg g^{-1} TSS, the CST of dredged sediment decreased from 92.4 s to 6.2 s and then increased to 7.9 s, and the SRF decreased from 42.1 × 10^{11} m kg^{-1} to 2.73 × 10^{11} m kg^{-1} and then increased to 6.47 × 10^{11} m

© 2024 The Author(s). Published by the Royal Society of Chemistry

Open Access Article. Published on 31 May 2024. Downloaded on 1/31/2026 4:51:15 PM.
This article is licensed under a Creative Commons Attribution-NonCommercial 3.0 Unported Licence.

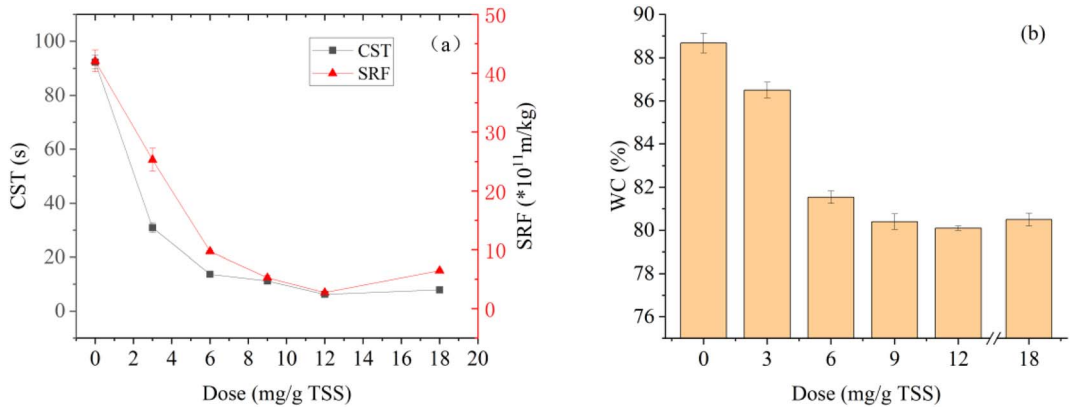

Fig. 3 Variations in (a) SRF, CST, and (b) WC of dredged sediment at different St-CTA dosages.

kg^{-1} (Fig. 3a). The WC of filter cakes also shows a similar trend (Fig. 3b). With the increase of St-CTA dosage from 0 to 12 mg g^{-1} TSS to 18 mg g^{-1} TS, the WC of the sediment cakes dropped from 88.7% to 80.1% and then rose to 80.5%.

SRF and CST can measure the filtration performance of dredged sediment, while the WC of filter cake can be used to measure the dewatering degree of sediment.[33,37] Therefore, the experimental result implied that St-CTA could significantly improve the filtration performance and dewatering degree of dredged sediment. However, when the dosage of St-CTA exceeded the optimal dosage of 12 mg g^{-1} TSS, the filtration performance of dredged sediment deteriorated. This was attributed to the result of the action of charge neutralization and reversal, which would be discussed further in Section 3.3. Hence, 12 mg g^{-1} TSS was determined as the optimal St-CTA dosage, under which the SRF, CST, and WC of the dredged sediment were reduced by 93.3%, 93.5%, and 9.7%, respectively.

3.3 Dose effects of St-CTA on pH, zeta potential, turbidity and settling curve of dredging sediment supernatant of dredged sediment

Fig. 4 shows the supernatant turbidity, settling curves, pH, and zeta potential of the dredged sediment samples under different St-CTA dosages. St-CTA has a significant effect on the removal of turbidity in the supernatant (Fig. 4a). With the dosage of St-CTA increased from 0 to 12 mg g^{-1} TSS to 18 mg g^{-1} TSS, the turbidity of the supernatant rapidly decreased from 3869 NTU to 16.3 NTU and then increased to 139.4 NTU. Under the optimal dosage of St-CTA (12 mg g^{-1} TSS), the turbidity removal rate of the supernatant reached 99.6%. The electric neutralization effect and the adsorption bridging effect generated by St-CTA would trap the tiny particles suspended in the system, which were not easy to settle, resulting in settlement. The reduction of tiny particles suspended in the supernatant was beneficial to reducing the turbidity of the supernatant. Moreover, correlation analysis showed that turbidity of supernatant was significantly positively correlated with the SRF ($R > 0.86$, $p < 0.05$) and CST ($R > 0.97$, $p < 0.05$) of sediment. This was attributed to the lower likelihood of drainage pathway blockage during the filtration process in conditions of low turbidity.

Settling curves are widely used for analyzing the sedimentation process of a suspension.[38] The settling curve of the raw sediment is not shown in Fig. 4b, because the mud–water interface of the raw dredged sediment sample was indistinct after settling for 15 minutes. It could be considered that the raw dredged sediment did not settle within 15 minutes. Adding St-CTA could effectively enhance the settling rate of the dredged sediment. The larger and denser flocs enlarged the density difference between solid and liquid phases, promoting the solid–liquid separation by gravity settling.[39] Noticeably, the fastest settling velocity corresponded to the lowest SRF, CST, and WC of dredged sediment. Improved settling capability enhances the efficiency of the filtrate discharge process, significantly increasing feed rate and raw material sedimentation.[40] However, excessive St-CTA led to a decline in sediment settlement rate.

The addition of St-CTA results in slight fluctuations in the pH of the dredged sediment, consistently maintaining it around 7.5 (Fig. 4c). This stability was attributed to the near-neutral pH of the St-CTA solution itself, which prevented significant alterations in the system's pH when introduced to the dredged sediment. Such consistency offered convenience in the subsequent treatment processes for both the dredged sediment and the resultant leachate.

Zeta potential is an important factor affecting the dispersion or aggregation of particles.[41] Thus, zeta potential is also an important indicator affecting the dewatering performance of dredged sediment. As shown in Fig. 4d, as the dosage of St-CTA increases from 0 to 12 mg g^{-1} TSS and then to 18 mg g^{-1} TSS, the zeta potential of dredged sediment increases from −13.6 mV to −4.5 mV until the surface charge of the dredged sediment shifts from negative to positive to 7.7 mV. The negative charge on the surface of the sediment particles enhanced the stability of the flocs due to the repulsion force. The cationic groups in St-CTA neutralized the negative charge, facilitating the collision and aggregation of the flocs. However, excessive addition of St-CTA could also cause a reversal in the charge of sediment particles from negative to positive, increasing the

Open Access Article. Published on 31 May 2024. Downloaded on 1/31/2026 4:51:15 PM.
This article is licensed under a Creative Commons Attribution-NonCommercial 3.0 Unported Licence.

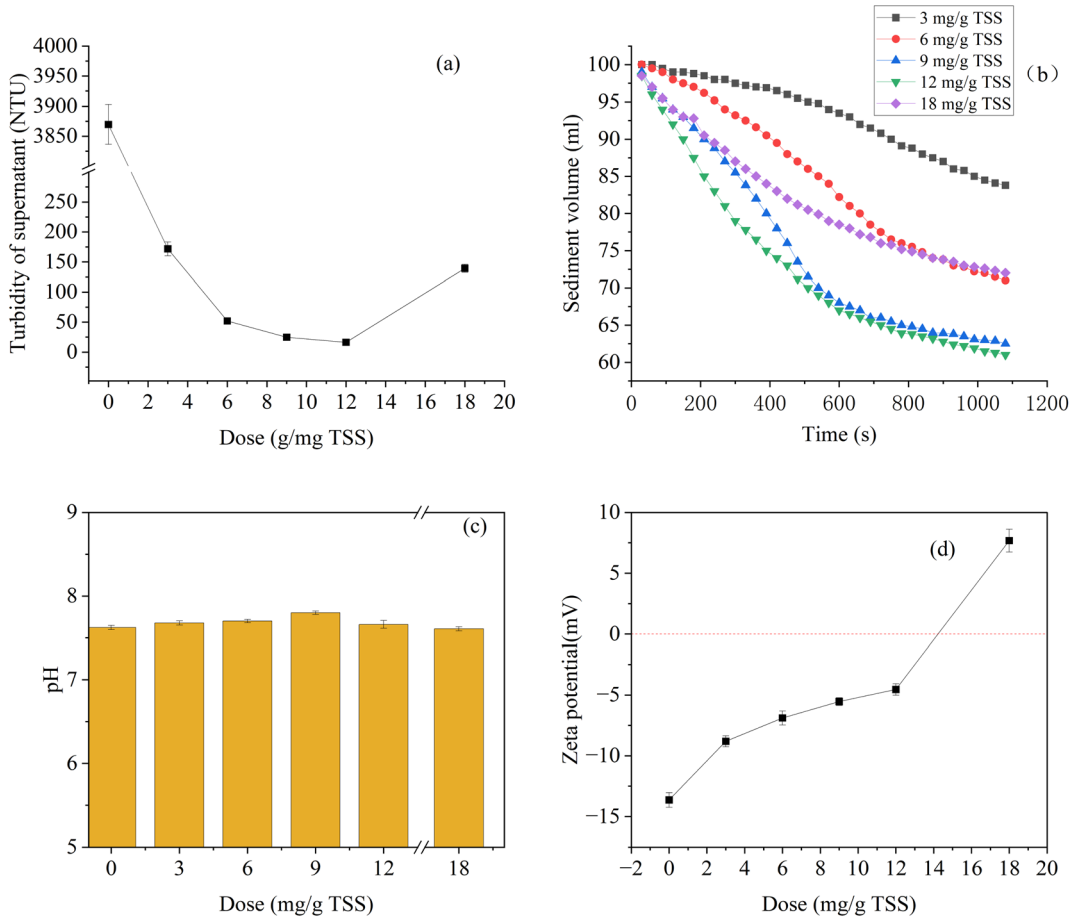

Fig. 4 Variations in (a) turbidity of supernatant after settling for 30 minutes and (b) settling rate of dredged sediment at different St-CTA dosages (c) pH and (d) zeta potential.

absolute value of the zeta potential. Studies have shown that a lower absolute value of the zeta potential corresponds to reduced interparticle charge repulsion, enhancing the dewaterability of the dredged sediment.[5] This also explained the deterioration of the dewatering performance of sediment caused by the excessive addition of St-CTA in this study.

3.4 Dose effects of St-CTA on particle size distributions and fractal dimension of dredged sediment

Fig. 5 demonstrates the particle size distribution and D50 of dredged sediment at different dosages of St-CTA. The particle size of sediment is regarded as an important parameter influencing sediment dewatering efficiency.[42] Fig. 5a demonstrates

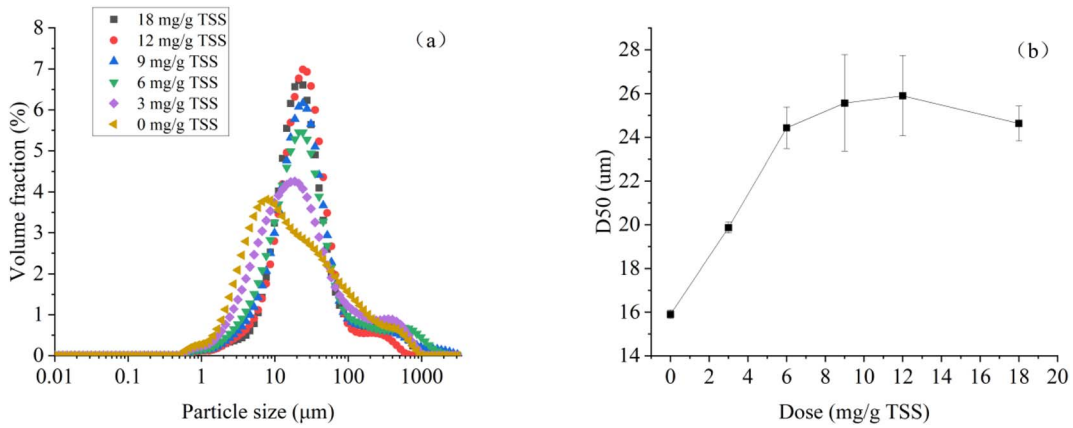

Fig. 5 Variations in (a) particle size distribution and (b) D50 of dredged sediment at different St-CTA dosages.

© 2024 The Author(s). Published by the Royal Society of Chemistry

Open Access Article. Published on 31 May 2024. Downloaded on 1/31/2026 4:51:15 PM.
This article is licensed under a Creative Commons Attribution-NonCommercial 3.0 Unported Licence.

that St-CTA has a significant impact on the particle size distribution of sediment. As shown in Fig. 5b, with the increase of St-CTA dosage from 0 to 12 mg g^{-1} TSS and then to 18 mg g^{-1} TSS, D50 of the sediment increases from 15.9 μm to 25.9 μm and then decreases to 24.6 μm, indicating a trend of initial increase followed by a decrease. Under the optimal dosage of St-CTA, the D50 of the sediment increased by 62.9%. In addition, correlation analysis showed that D50 was significantly negatively correlated with the SRF ($R < -0.99$, $p < 0.01$), CST ($R < -0.94$, $p < 0.01$), and WC ($R < -0.98$, $p < 0.01$) of sediment, aligning with previous research results.[43] Big flocs promoted the formation of large gaps and tunnels for drainage, resulting in an improved dewatering rate and low water content in sediment cakes.

The cationic groups of St-CTA neutralized the surface negative charge of the sediment particles, leading to destabilization and collision. At the same time, the cationic modified starch had a long linear chain architecture, enhancing its bridging effects,[44] which made it easier for the dredge sediment particles to flocculate into large flocs. However, when St-CTA was used in excess, the overabundance of positive charges on the floc surfaces could cause a re-stabilization effect.[45] As the absolute value of the surface charge of the sediment particles rose, the repulsive force between particles intensified, making the formation of large flocs more challenging.

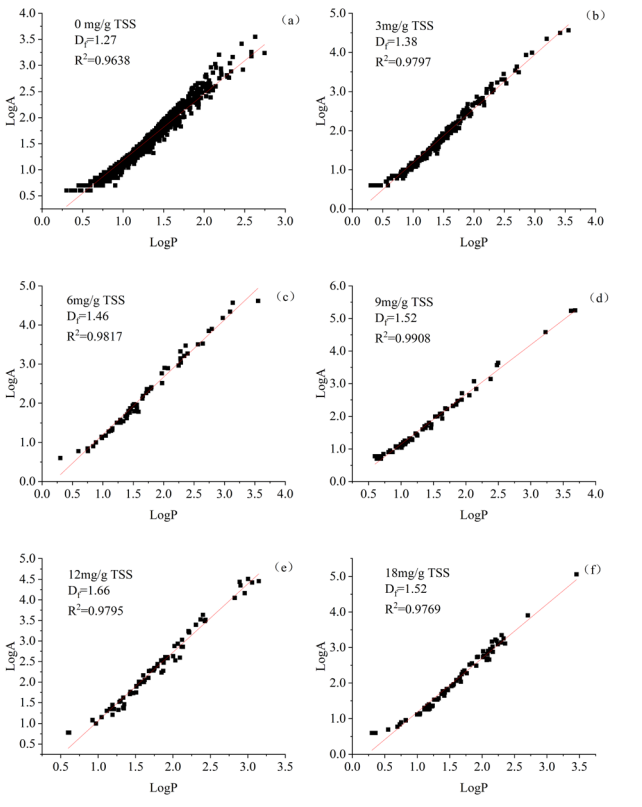

Fig. 6 Calculation process and results of the fractal dimensions (D_f) of dredged sediment with the addition of St-CTA at dosages of (a) 0 mg g^{-1} TSS, (b) 3 mg g^{-1} TSS, (c) 6 mg g^{-1} TSS, (d) 9 mg g^{-1} TSS, (e) 12 mg g^{-1} TSS, and (f) 18 mg g^{-1} TSS. R^2 represents the correlation coefficient of the linear fit.

3.5 Dose effects of St-CTA on the fractal dimension of dredged sediment

Fig. 6 shows the calculation process and results of the fractal dimension (D_f) of sediment particles at different St-CTA dosages. With the dosage of St-CTA increased from 0 to 12 mg g^{-1} TSS to 18 mg g^{-1} TSS, the fractal dimension of flocs rose from 1.27 to 1.66 and then decreased to 1.52. The addition of St-CTA significantly elevated the fractal dimension of the sediment floc. It was reported that the flocculation process with larger fractal dimensions produced denser flocs.[25] Besides, correlation analysis showed that the fractal dimension was significantly negatively correlated with the SRF ($R < -0.92$, $p < 0.01$), CST ($R < -0.85$, $p < 0.05$), and WC ($R < -0.90$, $p < 0.05$) of dredged sediment, indicating that denser sediment particles contributed to better dewatering performance. Obviously, the conditioning of St-CTA made the flocs of dredged sediment more dense. Due to the electrostatic repulsion of cationic groups inside molecules, St-CTA presented a rigid linear structure in water with low steric hindrance, and the stability of the six-carbon sugar structure enabled St-CTA to serve as a skeleton for flocs,[46] facilitating the formation of denser flocs during the flocculation process. The relationship between the fractal dimension and the dewatering performance of dredged sediment showed that the compact floc could reduce the compressibility of the filter cake, preventing the collapse of drainage channels within the filter cake and thereby improving its dehydration performance and degree of dewatering.

3.6 Dose effects St-CTA on microscopic morphology of dredged sediment

Fig. 7 illustrates the microscopic morphology of dredged sediment flocs under different dosages of St-CTA, revealing that the addition of St-CTA significantly alters the microstructure of dredged sediment surfaces. Fig. 7a shows that the microscopic surface shape of the raw dredged sediment is smooth, and numerous regular lamellar aggregations, mainly related to illite and quartz, are observed.[47] It was obvious that pores or channels were difficult to form on raw sediment. With the addition of St-CTA, the microstructure surface morphology of the sediment gradually became rough and discontinuous. Fig. 7e demonstrates that, at the optimal dosage of St-CTA, the sediment surface is roughest, with aggregates forming, which is conducive to the creation of channels for releasing water trapped within the sediment.[48] Fig. 7f shows that excessive addition of St-CTA leads to a decrease in the roughness of the sediment surface and a reduction in agglomerates, pores, and drainage channels.

3.7 Dose effects of St-CTA on rheology of dredged sediment

Rheology refers to the deformation and flow properties of substances under the action of external forces. It means that rheological indicators can produce significant information about sediment transport, handling, drying, and molding processes and may affect the mass, heat, mixing, and transport of sediments.[47] As shown in Fig. 8a, at lower shear rates, the

Open Access Article. Published on 31 May 2024. Downloaded on 1/31/2026 4:51:15 PM.
This article is licensed under a Creative Commons Attribution-NonCommercial 3.0 Unported Licence.

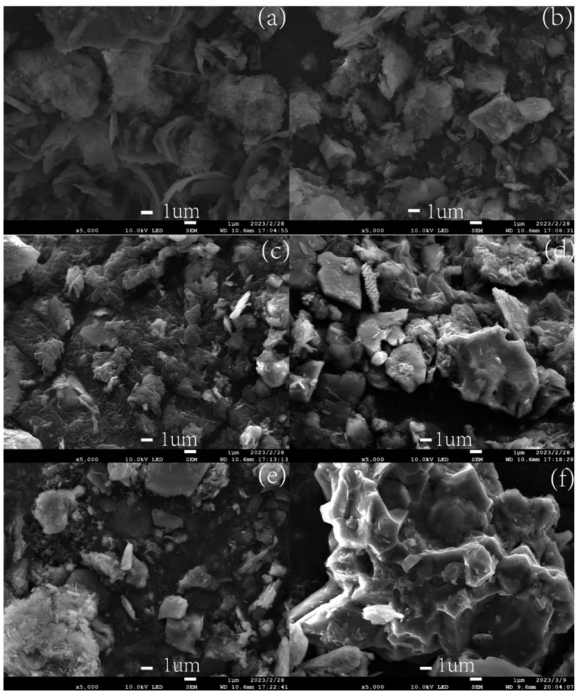

Fig. 7 The microscopic morphological changes of dredged sediment surface with the addition of St-CTA as (a) 0 mg g^{-1} TSS, (b) 3 mg g^{-1} TSS, (c) 6 mg g^{-1} TSS, (d) 9 mg g^{-1} TSS, (e) 12 mg g^{-1} TSS, and (f) 18 mg g^{-1} TSS.

viscosity of dredged material gradually declines with the rise in shear rate, indicating that the sediment behaves as a non-Newtonian fluid exhibiting shear-thinning properties. Nevertheless, at higher shear rates, the viscosity of the sediment slowly increases, demonstrating shear-thickening behavior. At lower shear rates, the sediment belongs to Bingham fluid.[49] When the dosage of St-CTA increased from 0 to 12 mg g^{-1} TSS, the viscosity of the sediment increased slightly. This is because the rigid long chain of St-CTA produced the effect of adsorption/bridge, promoted reticular colloid structure formation, and enhanced the viscosity of sediment. When the dosage of St-CTA increased to 18 mg g^{-1} TSS, the excessive positive charge caused an increase in the electrostatic repulsion among sediment particles and the excess starch molecules condensing and intertwining in the system, which further increased the viscosity of the sediment. However, at high shear rates, starch molecular chains disentangle and stretch, leading to the disruption of the floc structure.

Shear stress is influenced by interparticle forces such as van der Waals forces, electrostatic forces, and frictional forces.[49,50] As shown in Fig. 8b, after St-CTA conditioning, the shear force of the sediment increases, especially at high shear rates. Combined with the observations from Fig. 5 and 7, the addition of St-CTA led to an increase in the size of sediment flocs and a rougher surface morphology, resulting in increased friction between particles. In this case, the friction significantly exceeded the electrostatic and van der Waals forces acting on the flocs of sediment, giving rise to an increase in the shear stress. Furthermore, the flowability of the sediment conditioned with St-CTA worsened, which was attributed to the formation of flocculation after conditioning. It is essential to consider the risk of blockages in pipeline transport due to the reduced flowability of conditioned sediment.

3.8 The effects of St-CTA on EPS of dredged sediment

The 3D-EEM (Three-Dimensional Excitation Emission Matrix) method serves as an analytical approach to characterize natural organic matter.[51] Extracellular polymeric substances (EPS) in sediment can be categorized into three distinct layers: soluble EPS (S-EPS), which are soluble in water or freely exist in the sediment suspension; loosely bound EPS (LB-EPS), which are located on the outer surface of the cell and are not tightly bound to the cell; and tightly bound EPS (TB-EPS), which are closely attached to the microbial cell surface. As shown in Fig. 9a, upon visual inspection, two main fluorescent peaks were identified in the S-EPS layer of the original sediment: peak A (Ex/Em = 290 : 320), associated with soluble microbial byproducts, and peak B (Ex/Em = 315 : 400), linked to humic acids. Similarly, the LB-EPS layer exhibited two distinctive peaks: peak C (Ex/Em = 285 : 315), associated with soluble microbial byproducts, and peak D (Ex/Em = 340 : 430), associated with humic acids. In the

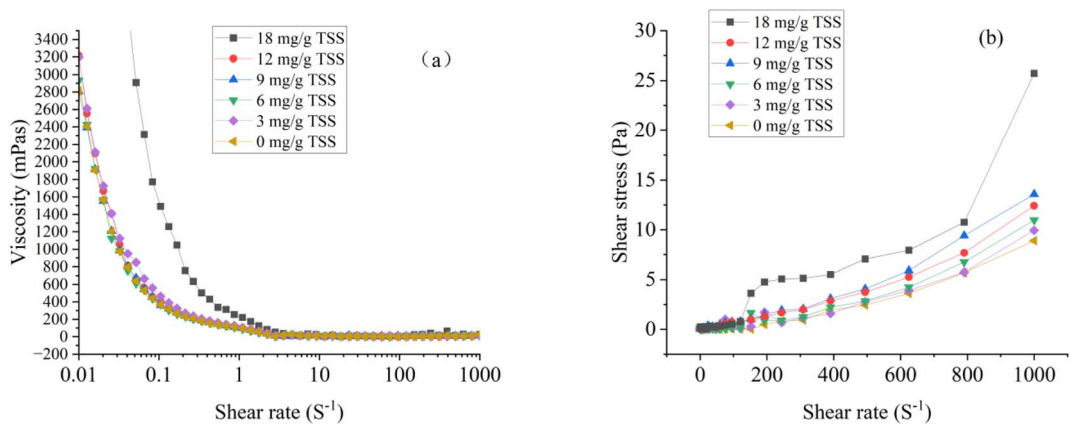

Fig. 8 Variations in (a) viscosity, (b) shear stress with shear rate of dredged sediment at different St-CTA dosage.

© 2024 The Author(s). Published by the Royal Society of Chemistry

Open Access Article. Published on 31 May 2024. Downloaded on 1/31/2026 4:51:15 PM.
This article is licensed under a Creative Commons Attribution-NonCommercial 3.0 Unported Licence.

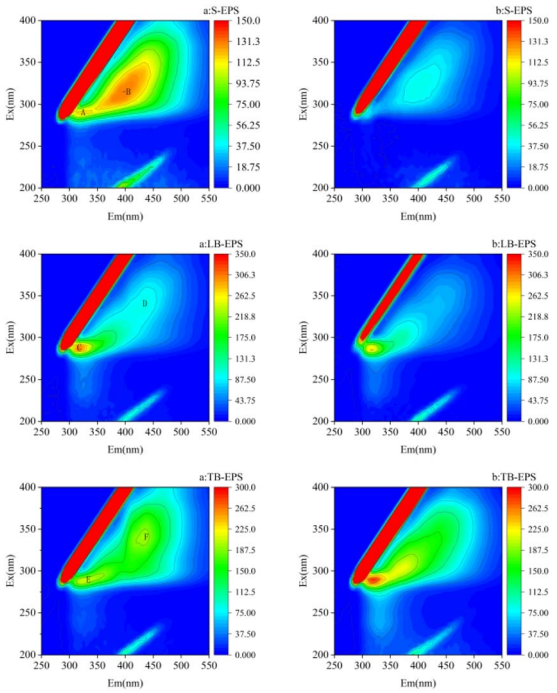

Fig. 9 Three-dimensional (3D) fluorescence spectra of the S-EPS, LB-EPS and TB-EPS of (a) raw sediment, (b) the conditioned sediment with St-CTA dosage of 12 mg g^{-1} TSS.

TB-EPS layer, two characteristic peaks were observed: peak E (Ex/Em = 290 : 330), linked to soluble microbial byproducts, and peak F (Ex/Em = 340 : 435), associated with humic acids. As shown in Fig. 9b, under the optimal St-CTA dosage of 12 mg g^{-1} TSS, fluorescence intensity decreased in the S-EPS and LB-EPS layers, indicating a reduction in EPS concentration, while an increase in fluorescence intensity of peak E and a decrease in peak F were observed in TB-EPS. St-CTA exhibited surfactant properties, neutralizing the negative surface charge of sediment through surfactant adsorption, which implied that St-CTA could bind with both loosely bound extracellular polymeric substances (LB-EPS) and tightly bound extracellular polymeric substances (TB-EPS) in the sediment. This weakened the binding force between sediment flocs LB-EPSs and TB-EPSs, facilitating EPS dissolution.[52] Simultaneously, a portion of organic matter from S-EPS and LB-EPS is converted to TB-EPS.[53] Related studies suggested that the decrease in S-EPS and LB-EPS concentrations contributed to the enhancement of sediment filtration performance.[34,54]

4 Conclusions

In this paper, a potentially environmentally friendly cationic starch St-CTA was successfully prepared for the flocculation dewatering of dredged sediment. This study demonstrates that St-CTA, a type of etherified starch, can serve as an excellent conditioning agent for sediment dewatering. Under the optimal St-CTA dosage (12 mg g^{-1} TSS), the dewatering capacity of dredged sediment was greatly improved, and the SRF, CST, and WC were reduced by 93.3%, 93.5%, and 9.7%, respectively. At the same time, the zeta potential, turbidity of supernatant, fractal dimension, particle size, and other characteristics of dredged sediment had obviously changed. The findings of this research broaden our understanding of St-CTA's treatment of dredged sediment dewatering, thereby facilitating the development of promising strategies for deep dewatering/filtration of dredged sediments in the future.

Author contributions

Shilei Tang: conceptualization, methodology, formal analysis, data curation, writing – original draft. Shaobin Huang: conceptualization, supervision, funding acquisition. Pengfei Chen: writing – review & editing, methodology. Zhipeng Wu: writing – review & editing. Tianyu Zhao: methodology.

Conflicts of interest

The authors declare that they have no known competing financial interests or personal relationships that could have appeared to influence the work reported in this paper.

Acknowledgements

This research was financially supported by Research Project of Guangxi Provincial Department of Science and Technology Department (No. GuiKe AD23026330 and No. GuiKe AB23026119), National Natural Science Foundations of China (No. 52270105), Science and Technology Innovation Program from Water Resources of Guangdong Province (No. 2023-03).

References

1 D. Wang, N. E. Abriak and R. Zentar, *Mar. Georesour. Geotechnol.*, 2016, **35**, 472–480.
2 R. Zentar, M. Miraoui, N. E. Abriak and M. Benzerzour, *Drying Technol.*, 2011, **29**, 1705–1713.
3 N. Yang, H. Xiao, K. Pi, J. Fang, S. Liu, Y. Chen, Y. Shi, H. Zhang, A. R. Gerson and D. Liu, *Chemosphere*, 2021, **269**, 129403.
4 N. Manap and N. Voulvoulis, *J. Environ. Manage.*, 2015, **147**, 338–348.
5 Y.-L. Chi, L.-F. Guo, Y. Xu, J.-W. Liu, W. Xu and H.-Z. Zhao, *Sep. Purif. Technol.*, 2018, **205**, 169–175.
6 M. Shi, G. Wen, H. Liu, G. Jian and Y. Chen, *Environ. Sci. Pollut. Res. Int.*, 2019, **26**, 17183–17194.
7 H. Zhou, W. Zhang, L. Li, M. Zhang and D. Wang, *Sci. Total Environ.*, 2021, **787**, 147703.
8 Q. Wei, X. Liu, Y. Zhang, K. Zhang, Z. Li, Z. Shen and C. W. K. Chow, *J. Environ. Chem. Eng.*, 2021, **9**, 104899.
9 L. Wang, L. Chen, D. C. W. Tsang, J.-S. Li, K. Baek, D. Hou, S. Ding and C.-S. Poon, *J. Cleaner Prod.*, 2018, **199**, 69–76.
10 P. Wu, K. Pi, Y. Shi, P. Li, Z. Wang, H. Zhang, D. Liu and A. R. Gerson, *Environ. Res.*, 2020, **184**, 109335.
11 L. Li, Z. Song, W. Zhang, H. Wu, W. Liu, J. Yu and D. Wang, *Colloids Surf., A*, 2021, **630**, 127514.

Open Access Article. Published on 31 May 2024. Downloaded on 1/31/2026 4:51:15 PM. This article is licensed under a Creative Commons Attribution-NonCommercial 3.0 Unported Licence.

12 M. M. Khachan and S. K. Bhatia, *Geotextiles and Geomembranes*, 2017, **45**, 280–293.
13 Z. Song, H. Gao, W. Liu, L. Li, W. Zhang and D. Wang, *J. Environ. Sci.*, 2021, **103**, 311–321.
14 D. J. Lee and Y. H. Hsu, *Water Environ. Res.*, 1995, **67**, 310–317.
15 H. Wei, B. Gao, J. Ren, A. Li and H. Yang, *Water Res.*, 2018, **143**, 608–631.
16 S. K. Dentel, M. M. Abu-Orf and C. A. Walker, *Chem. Eng. J.*, 2000, **80**, 65–72.
17 S. C. Sumner, C. C. Williams, R. W. Snyder, W. L. Krol, B. Asgharian and T. R. Fennell, *Toxicol. Sci.*, 2003, **75**, 260–270.
18 S. Bratskaya, S. Schwarz and D. Chervonetsky, *Water Res.*, 2004, **38**, 2955–2961.
19 B. S. Kaith, R. Jindal, A. K. Jana and M. Maiti, *Bioresour. Technol.*, 2010, **101**, 6843–6851.
20 R. Yang, H. Li, M. Huang, H. Yang and A. Li, *Water Res.*, 2016, **95**, 59–89.
21 Y. Chen, S. Liu and G. Wang, *Chem. Eng. J.*, 2007, **133**, 325–333.
22 R. N. Tharanathan, *Crit. Rev. Food Sci. Nutr.*, 2005, **45**, 371–384.
23 R. J. Anthony and R. C. Sims, *Carbohydr. Polym.*, 2013, **98**, 1409–1415.
24 S. Lv, T. Sun, Q. Zhou, J. Liu and H. Ding, *Carbohydr. Polym.*, 2014, **103**, 285–293.
25 H. Wu, Z. Liu, H. Yang and A. Li, *Water Res.*, 2016, **96**, 126–135.
26 M. Huang, Y. Wang, J. Cai, J. Bai, H. Yang and A. Li, *Water Res.*, 2016, **98**, 128–137.
27 S. Mishra, A. Mukul, G. Sen and U. Jha, *Int. J. Biol. Macromol.*, 2011, **48**, 106–111.
28 Z. Yang, H. Wu, B. Yuan, M. Huang, H. Yang, A. Li, J. Bai and R. Cheng, *Chem. Eng. J.*, 2014, **244**, 209–217.
29 S. Pal, D. Mal and R. P. Singh, *Carbohydr. Polym.*, 2005, **59**, 417–423.
30 Z. Liu, M. Huang, A. Li and H. Yang, *Water Res.*, 2017, **119**, 57–66.
31 W. Zhang, Z. Chen, B. Cao, Y. Du, C. Wang, D. Wang, T. Ma and H. Xia, *Water Res.*, 2017, **110**, 102–111.
32 M. Niu, W. Zhang, D. Wang, Y. Chen and R. Chen, *Bioresour. Technol.*, 2013, **144**, 337–343.
33 Y. G. Chen, H. Z. Yang and G. W. Gu, *Water Res.*, 2001, **35**, 2615–2620.
34 X. Y. Li and S. F. Yang, *Water Res.*, 2007, **41**, 1022–1030.
35 G. C. Bushell, Y. D. Yan, D. Woodfield, J. Raper and R. Amal, *Adv. Colloid Interface Sci.*, 2002, **95**, 1–50.
36 Z.-s. Cai, Z.-q. Song, S.-b. Shang and C.-s. Yang, *Polym. Bull.*, 2007, **59**, 655–665.
37 Y. Li, F. Yang, S. Miao, D. Wang, Z. Li, X. Yuan, L. Yuan and Q. Liu, *Chem. Eng. J.*, 2021, **405**, 126847.
38 X. Kang, Z. Xia, J. F. Wang and W. Yang, *Colloids Surf., A*, 2019, **579**, 123647.
39 D. Mowla, H. N. Tran and D. G. Allen, *Biomass Bioenergy*, 2013, **58**, 365–378.
40 Q. Zhang, M. Liu, J. Yin, C. Yuan, X. Mao, G. Hong, Y. Wang, F. Yang, F. Li and J. Li, *Journal of Water Process Engineering*, 2024, **57**, 104632.
41 Y. Li, Y. Zhu, D. Wang, G. Yang, L. Pan, Q. Wang, B. J. Ni, H. Li, X. Yuan, L. Jiang and W. Tang, *Water Res.*, 2020, **174**, 115626.
42 B. Jin, B.-M. Wilén and P. Lant, *Chem. Eng. J.*, 2003, **95**, 221–234.
43 D. Ge, W. Zhang, H. Yuan and N. Zhu, *J. Cleaner Prod.*, 2019, **241**, 118287.
44 P. Hu, S. Zhuang, S. Shen, Y. Yang and H. Yang, *Water Res.*, 2021, **189**, 116578.
45 W. Zhang, P. Xiao, Y. Liu, S. Xu, F. Xiao, D. Wang and C. W. K. Chow, *Sep. Purif. Technol.*, 2014, **132**, 430–437.
46 H. Wei, J. Ren, A. Li and H. Yang, *Chem. Eng. J.*, 2018, **349**, 737–747.
47 Z. Song, W. Zhang, H. Gao and D. Wang, *Sci. Total Environ.*, 2020, **739**, 139884.
48 H. Liu, H. Xiao, B. Fu and H. Liu, *Chem. Eng. J.*, 2017, **313**, 655–662.
49 N. Roussel, A. Lemaître, R. J. Flatt and P. Coussot, *Cem. Concr. Res.*, 2010, **40**, 77–84.
50 J. Hu and K. Wang, *Constr. Build. Mater.*, 2011, **25**, 1196–1204.
51 F. Lin, X. Zhu, Y. Luo, P. Yu and M. Liu, *RSC Adv.*, 2019, **9**, 6936–6945.
52 R. Guan, X. Yuan, Z. Wu, H. Wang, L. Jiang, Y. Li and G. Zeng, *Sci. Total Environ.*, 2017, **609**, 1433–1442.
53 S. Shen, W. Xia, Z. Luo, Y. Pan, P. Hu, L. Zhang, H. Shi and H. Yang, *Chemosphere*, 2023, **344**, 140323.
54 B. Cao, W. Zhang, Q. Wang, Y. Huang, C. Meng and D. Wang, *Water Res.*, 2016, **105**, 615–624.

© 2024 The Author(s). Published by the Royal Society of Chemistry